9-1-2010

Association Between Chronic Liver and Colon Inflammation During the Development of Murine Syngeneic Graft-Versus-Host Disease

Jason Anthony Brandon
University of Kentucky, jabran2@email.uky.edu

Jacqueline Perez-Rodriguez
University of Kentucky, jprjackie@yahoo.com

C. Darrell Jennings
University of Kentucky, cdjenn@email.uky.edu

Donald A. Cohen
University of Kentucky, don.cohen@uky.edu

Vishal J. Sindhava
University of Kentucky, vjsind2@uky.edu

See next page for additional authors

Notes/Citation Information
Published in *American Journal of Physiology: Gastrointestinal and Liver Physiology*, v. 299, issue 3, p. G602-G613.

Digital Object Identifier (DOI)
https://doi.org/10.1152/ajpgi.00511.2009

Articles in PresS. Am J Physiol Gastrointest Liver Physiol (July 15, 2010). doi:10.1152/ajpgi.00511.2009

Association between chronic liver and colon inflammation during the development of murine syngeneic graft-versus-host disease.

J. Anthony Brandon[1,4], Jacqueline Perez[5], C. Darrell Jennings[2], Donald A. Cohen[1,5], V.J. Sindhava[1], S. Bondada[1,4], Alan M. Kaplan[1,4,5] and J. Scott Bryson[1,3,4,5].

[1]Department of Microbiology Immunology and Molecular Genetics, [2]Pathology, [3]Internal Medicine, [4]Markey Cancer Center and [5]Graduate Center for Toxicology, University of Kentucky Medical Center, Lexington, KY, 40536

Running Head: IBD-associated chronic liver inflammation.

Contact information: Dr. J. Scott Bryson, Department of Internal Medicine, Division of Hematology, Oncology and Blood & Marrow Transplantation, 108B Combs Cancer Research Building, University of Kentucky, 800 Rose Street, Lexington, Kentucky 40536.

Email: jsbrys@.uky.edu

ABSTRACT

The murine model of cyclosporine A (CsA)-induced syngeneic graft-versus-host disease (SGVHD) is a bone marrow transplantation (BMT) model that develops chronic colon inflammation identical to other murine models of $CD4^+$ T cell-mediated colitis. Interestingly, SGVHD animals develop chronic liver lesions that are similar to the early peribiliary inflammatory stages of clinical chronic liver disease which is frequently associated with inflammatory bowel disease (IBD). Therefore, studies were initiated to investigate the chronic liver inflammation that develops in the SGVHD model. To induce SGVHD, mice were lethally irradiated, reconstituted with syngeneic BM and treated with CsA. All of the SGVHD animals that developed colitis also develop chronic liver inflammation. Liver samples from control and SGVHD animals were monitored for tissue pathology, RNA for inflammatory mediators and phenotypic analysis and *in vitro* reactivity of the inflammatory infiltrate. Diseased animals developed lesions of intra- and extrahepatic bile ducts. Elevated levels of mRNA for molecules associated with chronic liver inflammation including mucosal cellular adhesion molecule -1, the chemokines CCL25, CCL28, CCR9 and T_H1 and T_H17 associated cytokines were observed in livers of SGVHD mice. $CD4^+$ T cells were localized to the peribiliary region of the livers of diseased animals and an enhanced proliferative response of liver associated mononuclear cells against colonic bacterial antigens was observed. The murine model of SGVHD colitis may be a valuable tool to study the entero-hepatic linkage between chronic colon inflammation and inflammatory liver disease.

KEY WORDS*: chronic liver inflammation, inflammatory bowel disease, T_H1 immunity, T_H17 immunity,*

INTRODUCTION

Clinically a high percentage of IBD patients also present with some form of portal/periportal liver inflammation including autoimmune hepatitis (AIH), primary sclerosing cholangitis (PSC) and occasionally primary biliary cirrhosis (PBC) (30). In a recent study, elevation of serum aminotransferase was found in one third of 500 IBD patients (39). Primary sclerosing cholangitis and AIH are common extraintestinal manifestations of IBD, with the majority of PSC patients having IBD (>75%); ulcerative colitis is present in most (~90%), with Crohn's Disease being present in the rest (5, 17). While PSC is typically diagnosed after the diagnosis of IBD, the diagnosis of PSC can precede IBD by several years (30). Autoimmune hepatitis is a more classic autoimmune disease but some patients can be diagnosed with features of both PSC and AIH as an overlap disorder. These forms of chronic liver disease are characterized by portal/periportal inflammation that can lead to fibrosis.

IBD-associated chronic liver inflammation such as PSC appears to be mediated by IFN-γ-producing, microbial-antigen-specific $CD4^+$ T cells activated in the gut and recruited to the liver by aberrant expression of mucosal addressin cellular adhesion molecule 1 (MAdCAM-1) and chemokines (CCL25) that are typically expressed in the gut (reviewed (1)). Upregulation of these molecules on the portal endothelium of the liver enables the recruitment of $\alpha4\beta7^+$, $CCR9^+$, $CD4^+$ memory T cells to the liver from the gut (1). α4β7 and CCR9 are the ligands for MAdCAM and CCL25, respectively. It

has been postulated that Toll-like receptors (TLR) on immune (macrophages, Kuppfer cells, dendritic cells (DC)) and non-immune cells (cholangiocytes) in the liver are exposed to bacteria/bacterial products via entero-hepatic circulation and bind pathogen-associated molecular patterns (PAMPs), become activated and secrete proinflammatory cytokines and chemokines (TNF-α, IL-1β, IL-6; CCL25) (42) that can participate in the recruitment of adaptive immune cells to the liver (28).

Animal models have been developed to understand the pathophysiology associated with chronic liver inflammation. One class utilizes bacterial wall components and develop biliary sclerosis after bacterial overgrowth of the small bowel (35) or following injection of bacterial products and induction of experimental colitis in rats and rabbits (36). Non-suppurative destructive cholangitis is the main lesion during murine allogeneic GVHD (58). The injection of 2,4,6-trinitrobenzene sulphonic acid (TNBS) into the extra-hepatic bile duct induces an antigen-specific immune response that is similar to PSC clinically, including a $CD4^+$ T_H1 immune response with stricturing of hepatic bile ducts and induction of portal fibrosis (43). In addition to models of PSC, other murine models have been developed to simulate AIH. The intravenous injection of conconavilin A (32) or the injection of antigen-specific T cells into transgenic mice that express novel antigen on the surface of hepatocytes results in the development of T cell mediated AIH (11). More recently PBC was shown to develop in IL-2Rα$^{-/-}$ animals. In this model the $CD8^+$ effector cells differentiated in the liver and appeared not to be recruited from other sites (59).

Inflammatory bowel disease represents a chronic inflammation of the intestinal tract of unknown origin. It has been recognized that IBD results from a dysregulated immunological response to commensal bacteria in genetically susceptible individuals (48). Experimentally, colitis develops in chemically treated and gene knockout animals, and following adoptive transfer of naïve $CD4^+$ T cells into immune deficient recipients (reviewed (49)). The majority of these models have been thought to develop as a result of a T_H1 cytokine-based immune response that is characterized by excessive production of IL-12/IFN-γ/TNF-α. Recently, however, it has been shown that in addition to T_H1 cells, a distinct population of IL-17-producing $CD4^+$ T cells (T_H17 cells) can drive intestinal inflammation (reviewed (23)).

In murine SGVHD a colitis-like disease developed following lethal irradiation, syngeneic BMT and a short course of CsA therapy (7, 18, 19). Clinical symptoms (weight loss, diarrhea) typically occurred in 80-100% of the CsA-treated animals, with lymphocytic infiltration of the colon and liver being observed. *In vivo* depletion and adoptive transfer studies demonstrated that $CD4^+$, but not CD8+ T cells played a prominent role in the development of murine SGVHD-associated colitis (6, 10). Similar to murine colitis models, recent studies have demonstrated enhanced responsiveness of SGVHD $CD4^+$ T cells against antigens isolated from cecal bacterial preparations (6), leading to the speculation that $CD4^+$ T cells reactive against bacterial antigens mediate the chronic intestinal and liver inflammation observed during murine SGVHD.

There currently are no established animal models of IBD-associated chronic liver inflammation. In this manuscript, data is presented that demonstrates an absolute linkage between liver inflammation and colitis in the SGVHD model and test the hypothesis that microbial-specific T cells migrate from the colon to the liver to induce chronic liver inflammation. Chronic liver inflammation of intrahepatic/extrahepatic bile ducts was associated with the aberrant expression of colon-associated CAM/chemokines and a T_H1/T_H17 inflammatory immune response. Given the complete entero-hepatic linkage, the role of $CD4^+$ T cells in the SGVHD disease model and the similarity in inflammatory response/lesions with the early lesions associated with clinical PSC, murine SGVHD is a useful model in which to study the immune mechanisms that are essential for the initiation and maintenance of chronic liver inflammation during IBD.

MATERIALS and METHODS

Animals. Female C3H/HeN mice were purchased from Harlan (Indianapolis, IN) at 19-21 days of age and were used within 1 week of arrival. Animals were housed in sterile microisolator cages (Lab Products, Maywood, NJ) and were fed autoclaved food and acidified water *ad libitum*. All animal protocols were approved by the University of Kentucky Institutional Animal Care and Use Committee.

Induction of SGVHD. Bone marrow (BM) was isolated from the femurs and tibias of syngeneic age matched mice. Donor BM suspensions were prepared in RPMI 1640 (Cellgro, Herndon, VA) containing 100 U/ml penicillin and 100 µg/ml streptomycin and 2 mM glutamine (GIBCO, Grand Island, NY) and depleted of Thy-1^+ BM cells as previously described (8). To induce SGVHD, recipient mice were lethally irradiated (900 cGy) in a Mark I ^{137}Cs irradiator (J.L. Shepherd and Associates, Glendale, CA). Following irradiation, the animals were reconstituted i.v. with $5x10^6$ syngeneic T cell depleted BM (ATBM) cells, 4-6 h after conditioning. Beginning on the day of BMT, the mice were treated daily i.p. for 21 days with 15 mg/kg/day of CsA or the diluent olive oil (Sigma-Aldrich, St. Louis, MO). Upon cessation of CsA therapy, the BMT control and CsA-treated animals were weighed 3 times per week and monitored for the development of clinical symptoms of SGVHD (weight loss, diarrhea). Animals that developed clinical symptoms for three consecutive weighings were considered positive for the induction of SGVHD.

Histological Analysis of SGVHD Inflammation. Tissues were removed from euthanized animals at the indicated times after BMT and cessation of CsA therapy and placed into 10% buffered formalin. The fixed tissues were embedded in paraffin, cut into 4-6 μm sections, mounted onto glass slides and stained with a standard H&E protocol. All slides were analyzed blindly and were graded for inflammation according to a previously published grading scale (9).

Immunohistochemical Staining. Liver samples were taken and immediately embedded in Tissue-Tek Optimal Cutting Temperature (O.C.T.) Compound (Sakura Finetek, Torrance CA) and frozen in liquid nitrogen. Samples were then cut into 10-μm tissue sections, mounted on glass slides and stored in -20^{0}C freezer. Tissues were fixed with 3% paraformaldehyde for 15 minutes followed by 3 x 5 minute washes in PBS. Slides were blocked to prevent non-specific binding with 2 mg/ml normal donkey serum (Jackson ImmunoResearch, West Grove, PA), 0.3% Triton X-100 in PBS for 30 minutes 4°C. Slides were then incubated with FITC-conjugated mAb against CD4 (GK1.5; BD PharMingen, San Diego, CA) (1:1000) in PBS supplemented with 2 mg/ml normal donkey serum and 0.3% Triton X-100 at 4^{0}C overnight in a humidified chamber. Control staining was performed by using FITC IgG Rat antibody (1:1000). After 2 washes in PBS, the samples were visualized on a Carl Zeiss microscope 100x magnification and digitized with the camera AxioVision HR. Because the automatic exposure setting on the microscope camera overcompensated for tissues without T cell infiltration, post-capture image processing was used to adjust tissue section images to the equivalent levels of background fluorescence.

Quantification of Serum Markers. Serum/plasma ALT concentrations were performed as per manufactures instructions. Briefly 100 µl of serum was mixed with 1ml of 37^{o}C pre-warmed ALT (SGPT) reagent (Pointe Scientific, Canton, MI, USA) and further incubated at 37^{o}C for 1 minute before the absorbance at 340 nm was read. An additional 2 absorbance readings (340 nm) were taken 1 minute apart with the sample being incubated at 37^{o}C between readings. The ALT concentration (IU/L) was calculated by multiplying the average absorbance difference per minute (Δabs/min.) by the factor 1768.

Levels of anti-ssDNA in the serum/plasma of SGVHD mice were determined by ELISA. Briefly, wells of a 96-well plate were coated with 100 µl of ssDNA (heat denatured salmon sperm DNA at 10 µg/ml in citrate phosphate buffer, pH 5.0). The plates were incubated at 4°C overnight. After washing the plates were washed 2X with tris-buffered saline containing 0.3% Tween-20 (TBS-T (pH 7.6)). Plates were blocked with 1.0% BSA in TBS for 1 hour at room temperature. Plates were washed with TBS-T and experimental samples were diluted 1/20 in TBS-T containing 0.25% BSA and 100 µl were added per well for 2 hours at room temperature. (The standard positive control was pooled serum from (3H9 × CD5$^{-/-}$) F1 mice at different dilutions (4)). Plates were washed with TBS-T and alkaline phosphatase-conjugated goat anti-mouse Ig (heavy and light chain), diluted 1/1000 in TBS-T with 0.25% BSA was added to each well for 2 hours at room temperature. Plates were washed with TBS-T and 2X with TBS. p-nitrophenyl phosphate (pNPP) was diluted to 1 mg/ml in substrate buffer (Phenylamine

buffer, pH 9.8) and added to each well for 30 minutes at room temperature and the absorbance was read at 405 nm.

Detection of perinuclear anti-neutrophil cytoplasmic antibodies (p-ANCA) was performed on ethanol fixed human neutrophil substrate slides (INOVA Diagnostics, San Diego, CA). Substrate slides were placed in a humidified chamber and 20 ul of either sample serum/plasma, positive or negative controls (INOVA Diagnostics) was added to the corresponding wells and incubated for 30 minutes at room temperature. Slides were then washed twice in PBS. Mouse IgG anti-bodies were detected by FITC-conjugated goat anti-mouse IgG antibodies (Sigma, St. Louis, MO) or goat anti-human IgG antibodies for positive controls (Sigma). After 30 minute incubation the slides were washed twice in PBS and analyzed using a Carl Zeiss microscope at 200x magnification and digitized with the camera AxioVision HR. The grading of the p-ANCA results was determined by the level of fluorescence as described by the manufacturer. Depending on the intensity of the staining the sample was given a fluorescent grade. Intensity grading criteria for fluorescence is as follows; brilliant fluorescent staining of nucleus (grade 4), bright fluorescent staining of nucleus (grade 3), nuclear staining clearly distinguishable, but not bright green (grade 2), lowest specific fluorescence that allows the differentiation of the nucleus from the background staining (grade 1), no distinction between the nucleus and background staining (grade 0). For this study a sample that had been graded 2 to 4 was considered positive and those samples graded either 0 or 1 were considered negative for p-ANCA.

Analysis of Cytokine Gene Expression by Real-time PCR. Total mRNA was isolated from the livers using Trizol reagent (Invitrogen, Grand Island, NY). mRNA (1 μg) from each group was reverse-transcribed into cDNA using the Promega (Madison, WI) reverse transcription system. cDNA was suspended in 1x master mix (0.5U Platinum Taq (Invitrogen), 0.2 nM of each dNTP, 0.2 mM PCR buffer (Idaho Technology, Inc., Salt Lake City, UT), 1x SYBR green (Molecular Probes, Eugene, OR). The reaction volume was made to 10 μl with ddH_20. Primers for IL-12, IFN-γ, TNF-α (21), IL-17, IL-23p19, CCR9, CCL25, CCL28, MAdCAM-1 and GADPH (44) were purchased from Integrated DNA Technologies (Coralville, IA) and were used at 1 μM concentration. Real-time PCR was performed on a Roche Lightcycler (Roche Diagnostics, Indianapolis, IN). Reaction conditions were as follows: 1 min at 95^0C followed by 50 cycles of 6s at 95^0C, 10s at 60^0C and15s at 72^0C. All the primers listed were normalized to GADPH and their expression calculated by the comparative C_T method.

Isolation of Liver-Associated Mononuclear (LAM) Cells. Livers were isolated from control BMT or SGVHD mice at 2-4 weeks after cessation of CsA therapy and perfused with 5 ml digestion buffer (RPMI 1640, 5% FCS, 0.05% collagenase IV (Sigma), 0.002% DNAse I (Sigma-Aldrich) then single cell suspensions were prepared in digestion buffer. The liver homogenate was placed into 50 ml centrifuge tubes and placed in a 37^0C water bath for 40 min with intermittent shaking. The cells were washed twice and the pellet was resuspended in 32% Percoll and centrifuged for 20 min at 2000 rpm at room temperature. The pellet was treated with 0.83% Tris-buffered NH_4Cl to remove RBC. After washing the cells were placed into 10% complete RPMI (10% FCS, 100 U/ml

255 penicillin and 100 µg/ml streptomycin and 2 mM glutamine, $5x10^{-5}$ M of 2-ME) for use in
256 *in vitro* proliferation assay and flow cytometric analysis.
257
258 *Proliferation Assay*. A cecal bacterial antigen (CeAg) preparation was prepared
259 according the procedure described by Cong et al (13). Bone marrow-derived dendritic
260 cells (DC) were generated by culturing C3H/HeN BM cells in RPMI 1640 containing 5%
261 FCS, penicillin/streptomycin/glutamine, and 5 mM 2-ME containing 20 ng/ml of
262 recombinant murine GM-CSF. The non-adherent cells were removed on days 3 and 5
263 and GM-CSF containing media was added. At 8-10 days after initiation of culture, cecal
264 antigen-pulsed DC were prepared by incubation of DC over night with 200 mg/ml of
265 CeAg (6). This dose of CeAg was the minimal dose required to induce maximal
266 proliferative response of $CD4^+$ T cells from SGVHD animals. Furthermore, incubation of
267 the DC with CeAg resulted in the maturation of DC resulting in increased expression of
268 MHC class II and B7 costimulatory molecules (J.S. Bryson, unpublished observation).
269 To determine the proliferative capacity of LAM against bacterial antigens, 2×10^5 LAM
270 from control or SGVHD mice were cultured with 1×10^4 irradiated (2000 cGy) DC or
271 CeAg –pulsed DC in a 96 well flat bottomed plate. Proliferation was measured by the
272 addition of [^{3}H]-thymidine during the last 18 h of a 96 h culture.
273
274 *Flow Cytometry***.** LAM cells were harvested and placed into staining buffer (PBS
275 containing 1% FBS, 0.1% NaN_3). To minimize non-specific staining, cells were
276 incubated with Ab against CD16/CD32 (2.4G2, Fc Block®, BD PharMingen). The cells
277 were stained with antibodies against CD4 (RM-4-5) (Caltag, Burlingame, CA), CD8 (CT-
278 CD8, Caltag), CD11b (M1/70), CD11c (BD PharMingen), TLR2 (eBioscience, San

279 Diego, CA) or TLR5 (Imgenex, San Diego, CA) then analyzed by flow cytometry. To
280 detect invariant natural killer T cells (iNKT), LAM were stained with αβTCR (H57-597
281 (BD PharMingen)) and α-GalCer loaded CD1 tetramers or unloaded CD1 tetramers
282 (kindly provided by Dr Mitch Kronenberg, La Jolla Institute for Allergy and Immunology,
283 San Diego, CA)(38). To determine intracellular cytokine production isolated LAM were
284 placed in complete RPMI growth media and stimulated with anti-mouse CD3 ascites for
285 8 hours at 37^{o}C. 2 μM monensin (eBioscience) was added during the last 4 hours of
286 culture and the cells were harvested, counted and placed in staining buffer (PBS
287 containing 1% FCS, 0.1% NaN_3). To reduce nonspecific staining, cells were incubated
288 with Ab against CD16/CD32 (Fc Block). 1 x 10^6 cells were then stained with
289 fluorochrome-conjugated mAb against CD4 (Caltag Burlingame CA). Intracellular
290 staining for IL-17, IFN-γ and TNF-α was performed using an Intracellular Cytokine
291 Staining Kit (eBioscience, San Diego, CA) according to manufacturer's directions.
292 Stained cells were analyzed using a BD Biosciences FACSCalibur flow cytometer (San
293 Jose, CA).
294
295 *Statistical Analysis***.** Statistical differences between groups were determined
296 using Student's t test. Differences ≤ 0.05 were considered statistically different.
297

RESULTS

Chronic Liver Pathology Associated with SGVHD. In addition to $CD4^+$ T cell-mediated inflammation in the epithelium and lamina propria of the colon (Fig. 1B vs 1A)(8, 10) with similarity to that observed in other models of murine colitis, significant and reproducible chronic inflammatory lesions are observed in the livers of SGVHD mice. As opposed to other murine models of colitis where chronic liver inflammation was observed in ~30% of the animals (40), histological analysis of both the colons and livers of SGVHD mice showed an absolute correlation between colitis and liver inflammation (9/9 in the current study). As shown in Figure 1, the inflammation described for samples taken in the first 2-4 weeks (Fig. 1D) after induction of SGVHD resembles the initial portal stage of clinical PSC, with inflammation limited to the portal area with no fibrosis being present (50). The lesions demonstrated significant portal lymphoid infiltrates in and around the intra-hepatic bile ducts with cholangiocyte necrosis (Fig. 1D). Liver samples taken at 8 weeks after cessation of CsA therapy (Fig. 1E (H&E) and 1F (Trichrome)) show extension beyond the limiting plate, resembling the periportal stage (II) of PSC (50). In contrast, an occasional lymphocyte can be observed outside the bile ducts of transplant control animals (Fig.1C) with no significant inflammatory response being observed. Examination of the extrahepatic bile ducts taken from the SGVHD animals showed apoptotic changes along with the bile duct invasion by inflammatory cells (Fig 1H). Inflammatory debris was also present in the lumen as well as inflammatory cells being located in the surrounding adventitia. Minimal inflammation was detected in the extrahepatic bile ducts isolated from the control BMT animals (Fig 1G). As shown previously (9), a significantly higher pathology

grade was observed in the colon and livers obtained from the SGVHD vs BMT control animals (Fig. 2). Although slightly reduced in severity, similar changes and pathology grades were observed 1 week after cessation of CsA therapy, prior to clinical symptoms of SGVHD (J.S. Bryson, unpublished observations).

Similar to what is observed clinically in patients with chronic liver inflammation, elevated levels of ALT were observed in the serum/plasma from SGVHD versus control BMT animals (Fig. 3A left panel). These increases were associated with the liver pathology observed in these animals (Fig. 1, 2) and were significantly elevated in SGVHD mice. Similar to the increased presence of liver enzymes, significantly increased levels of the autoantibody, anti-ssDNA (Fig 3B left panel), and importantly, perinuclear ANCA (p-ANCA), was observed during active disease as well (92% vs 10%)(Fig. 3C left panel). No differences in the levels of ALT, anti-ssDNA or p-ANCA autoantibodies were observed between control and CsA-treated animals one week after cessation of CsA therapy. However, the levels of these mediators increased with time after cessation until they were significantly increased by 5-6 weeks after induction therapy (Fig. 3 A-C right panels). Changes in ALT and p-ANCA have been associated with the development of chronic liver and colon inflammation including AIH and PSC (52, 54, 61).

Phenotypic Analysis of LAM Isolated from SGVHD Animals. In addition to studies monitoring pathology and liver-associated inflammatory markers, preliminary studies were initiated to monitor phenotypic changes that occur in the cellular immune response in the SGVHD liver. Liver associated mononuclear cells were isolated from transplant

346 control and SGVHD mice and monitored for the presence of $CD4^+$, $CD8^+$, NKT cells,
347 macrophages and neutrophils. No significant change was observed in $CD4^+$, $CD8^+$ (Fig
348 4A) and neutrophils (J. Bryson, unpublished observations) between BMT controls and
349 SGVHD animals. However, while the number of $CD4^+$ T cells did not change,
350 immunohistochemistry analysis showed that $CD4^+$ T cells were primarily localized
351 around the hepatic bile duct in the SGVHD liver (Fig 4D; arrows) compared to being
352 more diffusely dispersed thought the BMT control liver (Fig 4C). In addition, while no
353 apparent changes in T cell numbers were observed in the SGVHD liver, a significantly
354 decreased proportion of iNKT cells staining with α-GalCer-CD1d tetramers, in LAM from
355 BMT control vs SGVHD mice (Fig 4E). These cells have been shown to be involved in
356 development of oral tolerance (29, 57) and increase in SGVHD mice that recover from
357 colitis (~30% of diseased animals) (J. Bryson, unpublished observations). Finally,
358 significantly increased percentages of $CD11b^+$ (Fig. 4F) or $CD11b^+GR\text{-}1^-$
359 myeloid/macrophage cells were observed in LAM from SGVHD vs control animals. As
360 activation of innate effector cells via signaling through Toll-Like Receptors (TLR) may
361 play a significant role in the generation of adaptive immunity and more pointedly in the
362 initial stages of PCS pathology (53), increases in macrophages may be significant in the
363 development in SGVHD-associated liver inflammation.
364
365 *TLR Expression in SGVHD*. Gram positive and Gram negative bacteria were
366 found in a significantly higher percentage of the livers from CsA-treated versus control
367 animals (18). As bacteria are a significant source of TLR ligands (Pathogen-associated
368 molecular patterns (PAMPs)) it is likely that liver macrophages (Kupffer cells) and other
369 tissue cells come into contact with PAMPs resulting in activation and secretion of

inflammatory mediators. Real time PCR studies demonstrated that mRNA for all TLRs (1-9) was increased in the liver and colon of SGVHD mice. Importantly, mRNA for four of the five TLR's that are associated with binding bacterial PAMPs, TLR-1 (J. Bryson, unpublished observations), 2, 5 and 9, were significantly increased (Supplementary Data, Fig. 1). Finally, while antibodies are not available for all TLR, flow cytometry studies were performed using antibodies against TLR-2 and TLR5 to determine the nature of the LAM cells expressing these TLR. A significant increase in TLR2 and 5 staining was found in $CD11b^+$ cells isolated from the livers of SGVHD versus control BMT animals (Supplementary Data, Fig. 2).

Increased Inflammatory Mediators in Livers of SGVHD Mice. It has been widely suggested that IBD-associated chronic liver inflammation is mediated by T_H1 $CD4^+$ T cells (42). Initial studies demonstrated that SGVHD-mediated colon inflammation could be mediated by T_H17 or T_H1 immune responses (Brandon et al. Development of a T_H17 immune response during the induction of murine syngeneic graft-versus-host disease, Submitted for publication). To determine the nature of the T helper immune response in the SGVHD liver, LAM were isolated from control and diseased animals, stimulated and analyzed for the production of IL-17 (T_H17) or IFN-γ (T_H1) by intracellular cytokine staining techniques. As shown in Figure 5A, significantly increased percentages of both IL-17- and IFN-γ-producing $CD4^+$ T cells were observed in LAM isolated from SGVHD versus control animals. To support and expand these findings, mRNA was isolated from control and SGVHD livers and analyzed by real time PCR for T_H17 and T_H1 cytokines and inflammatory mediators that are associated with mucosal/liver inflammation. In the SGVHD liver there was a significant increase in mRNA for IFN-γ

(p=0.0009) as previously published in this model (19) and as demonstrated clinically (42). Since T_H17 cells have been shown to be elevated in IBD (20, 27) and in the SGVHD liver (Fig 5A), we sought to monitor the levels of T_H17-associated cytokines. Real time PCR analysis of liver RNA demonstrated increased expression of mRNA for IL-17 (p=0.0075), IL-23p19 and TNF-α (Fig 5B). In addition, increased mRNA for IL-12p40 (Fig 5B), a subunit for both IL-23 and the TH1 cytokine IL-12 was found to be significantly increased in diseased livers as well. Finally inflammatory chemokines and chemokine receptors involved in mucosal T cell homing (CCL25, CCL28 and CCR9) (Fig 6 A, B and D) were also increased in the livers of SGVHD mice compared to control animals. The increase in the expression of mRNA for CCR9 was also associated with a significant increase in the expression of $CD4^+$ LAM expression CCR9 (Fig. 4B) isolated from SGVHD animals. In line with the increase in gut homing chemokines, mRNA for MAdCAM, a CAM that has been associated with aberrant homing of lymphocytes to the liver of PSC patients (1, 16) was also significantly elevated in the SGVHD liver (Fig 6B). A corresponding increase (p=0.0557) in the percentage of $CD4^+$ expressing the ligand for MAdCAM, β7 integrin, was observed in the LAM from diseased versus control animals (Fig. 4B). Thus, there was an increase in $CD4^+$ T cells in the SGVHD liver that have a phenotype typical of effector cells that are derived in the intestinal tract.

We have observed that at the end of the CsA therapy (d21 post-BMT), prior to the development of clinical symptoms, there are increases in the expression levels of mRNA for proinflammatory cytokines, chemokines and adhesion molecules in the colons of SGVHD animals (Perez et al. Accumulation of $CD4^+$ T cells in the colon of CsA-treated mice following myeloablative conditioning and bone marrow

transplantation. Submitted for publication). It is proposed that during PSC, $CD4^+$ T cells migrate to the liver following activation in the colon via aberrant hepatic expression of MAdCAM and CCL25 (1)(Fig. 6). To investigate when T cells migrate into the liver of CsA-treated animals, liver tissue isolated from CsA-treated/SGVHD and control animals at 14, 21 and 37 days after BMT was stained for $CD4^+$ T cells. $CD4^+$ T cells were rarely observed in livers from control or CsA-treated animals at 14 and 21 days after BMT (Fig. 7A). Conversely, $CD4^+$ T cells were easily detected around the bile ducts (arrow) of diseased animals (37 days or 2-3 wks post-CsA) as was shown in Figure 7A. Furthermore, based on PCR analysis, MAdCAM mRNA was not elevated at day 14 post-BMT (J. Bryson, unpublished observations) and both MAdCAM and CCL25 trended towards increased levels in the liver of CsA-treated mice by day 21 post-BMT (Fig. 7B). Together, these findings suggest that an ordered expression of chemokines and CAM results in the timed migration of $CD4^+$ T cells into the liver.

LAM from SGVHD Mice Display Increased Microbial Reactivity. Previous studies have demonstrated increased proliferation of peripheral SGVHD $CD4^+$ T cells against bacterial antigens (6). Since it is known that increased bacteria were present in the livers of CsA treated animals (18), studies were performed to analyze the anti-bacterial antigen-specific proliferation of LAM isolated from SGVHD mice. LAM isolated from the livers of SGVHD mice demonstrated a significantly enhanced proliferative response against cecal bacterial antigens compared to control liver cells ($p=0.0002$) (Fig.8).

DISCUSSION

Chronic inflammatory processes of the liver are frequently associated with IBD (30). The current study describes the pathogenesis of chronic liver lesions that develop during the induction of murine SGVHD. Murine SGVHD is a unique model of colon inflammation with 100% penetrance of chronic liver inflammation that involves intra- and extrahepatic bile ducts. SGVHD-mediated liver disease was associated with increased ALT and p-ANCA levels similar to clinical markers of chronic liver inflammation. Liver mRNA levels of molecules associated with chronic inflammation and lymphocyte migration were increased along with T_H1 and T_H17-associated immune responses. Finally, increased reactivity of hepatic LAM to colonic bacterial antigen- pulsed DC's was observed suggesting that in SGVHD, microbial antigen-specific T cells may be responsible for the chronic inflammation that is observed in the liver. The utilization of murine SGVHD provides an opportunity to study the immune responses involved in both the initiation and progression of IBD-associated chronic liver inflammation.

It has been suggested that the lymphocytic infiltration that is seen in IBD-associated liver inflammation is comprised of cells that were activated within the gut and have migrated to the liver, aided by the aberrant expression of gut homing molecules (1). Studies in the SGVHD model have shown that colon CAM expression is elevated during CsA-therapy as early as day 14 post-BMT and $CD4^+$ T cells begin to accumulate in the colon at this time as well. (Perez et al. Accumulation of $CD4^+$ T cells in the colon of CsA-treated mice following myeloablative conditioning and bone marrow transplantation. Submitted for publication)(10). While the basis for this early induction

of CAMs and T cell accumulation in the colon is not known at this time, we hypothesize that pretransplant radiation and CsA treatment in the early post BMT period result in the production of inflammatory mediators including TNF-α. At least two possibilities exist to explain the early proinflammatory response that occurs during the induction of SGVHD. First, both radiation and CsA have been shown to induce oxidative stress and transcription factors (14, 51, 60, 64) that could mediate the upregulation of inflammatory cytokines (12, 25, 34, 63). In addition to direct involvement in the production of inflammatory mediators, irradiation and CsA have been shown to damage the gut leading to increased leakage of bacteria (18). The interaction of TLR on innate effector cells with microbial products (PAMPs) is an alternative pathway that could focus the enhanced production of proinflammatory cytokines such as TNF-α within the colon, leading to increased expression of CAM and in accumulation of $CD4^+$ T cells in the colons of CsA-BMT animals. Why the expression of these molecules is delayed in the liver, is not clear at this time, but may relate to differences in the effects of the inductive therapy on the target organs. Based on real time PCR data, MAdCAM-1 mRNA was not elevated at day 14 post-BMT, but along with the chemokine, CCL25, trended towards increased levels in the livers of CsA-treated mice by day 21 post-BMT (Fig.7). Few, if any, $CD4^+$ T cells were observed in the livers in the early post-transplant period (days 14 or 21)(Fig. 7), but were observed during active disease (Figs.4, 7). Phenotypically, increased numbers of $CD4^+$ T cells expressing markers of intestinal-derived T cells, β7 integrin and CCR9, were found in the livers of SGVHD animals when compared to controls. Together, these findings suggest $CD4^+$ effector cells are activated in the intestinal tract and that an ordered migration of $CD4^+$ T cells from the colon into the liver of SGVHD animals exists.

Hepatic T lymphocytes found in IBD-associated liver inflammation express the $CCR9^+$ $\alpha_4\beta_7^+$ phenotype classically seen in lymphocytes that have been activated by gut DC's (2). Abnormal expression of the mucosal addressin, MAdCAM-1, along with the gut-associated chemokine CCL25 has been observed at elevated levels in the liver endothelium in PSC (1, 26) and provided a mechanism by which $CCR9^+$ T cells activated in the intestinal tract can migrate to the liver. The mechanisms by which these inflammatory molecules are upregulated in the liver are unknown but may involve the activation of TLR ligands with microbial PAMPS that arrive in the liver via entero-hepatic circulation resulting in the production of inflammatory mediators. Levels of TLR mRNA that bind bacterial PAMPS, as well as TLR-expressing myeloid LAM were elevated in livers from SGVHD animals (Supplementary Fig. 1, 2). This is supported further by previous data demonstrating that increased numbers of bacteria can be detected in the livers of CsA treated mice during the induction of SGVHD (18). Furthermore, similar to peripheral effector cells from diseased animals (6), the LAM's isolated from SGVHD mice demonstrated an increased proliferative response to bacterial antigen-pulsed APC. We have previously shown that isolated $CD4^+$ T cells from the peripheral lymphoid tissues of SGVHD mice could adoptively transfer colitis and liver inflammation into secondary recipient animals (6). The ability of LAM isolated from the livers of SGVHD mice to transfer disease to secondary recipient animals has yet to be determined.

Damage to liver bile ducts during IBD-associated liver inflammation is thought to be mediated by T_H1, $CD4^+$, IFN-γ-producing T cells. Hepatocellular damage through IFN-γ is thought to occur by a variety of mechanisms including direct cellular injury,

514 modulation of Ag presentation, and both the recruitment and activation of other immune
515 cells (15, 55). However, the immune phenotype of the cells that induce autoimmune
516 chronic liver inflammation has come into question, with T_H17 immunity being observed
517 as well (22, 45). Data presented here indicates that T_H17 cells, determined by
518 increased intracellular cytokine production of IL-17 by $CD4^+$ LAM and increased mRNA
519 levels of T_H17 associated cytokines (IL-17, IL-23p19, TNF-α), were increased in the
520 livers of SGVHD mice. We have also found a significant increase in T_H17 associated
521 cytokines in the colons of SGVHD mice (Brandon et al. Development of a T_H17 immune
522 response during the induction of murine syngeneic graft-versus-host disease, Submitted
523 for publication). This increase was observed even at day 21 post BMT in CsA-treated
524 mice suggesting that T_H17 T cells may have an important role in SGVHD-associated
525 colitis. As increased percentages of $CD4^+T_H1$ were also found in diseased livers, the
526 role that T_H17 and T_H1 $CD4^+$ T cells play during SGVHD-induced chronic liver
527 inflammation remains to be determined. It should be noted that while T_H17 cells are
528 present in the PBC livers of IL-2Rα$^{-/-}$ animals, a model of chronic liver inflammation, the
529 data suggests that the IL-17 secreting cells differentiate in the liver and appear not to be
530 recruited from other sites (33), with no enterohepatic linkage being observed in the
531 development of the autoimmune PBC. Finally, both T_H17 and T_H1 cells have both been
532 detected in an autoimmune model of skin inflammation. These cells developed with
533 different kinetics with T_H17 cells emerging early, being replaced by a T_H1 $CD4^+$ immune
534 response later in the disease process (37).

535 It is likely that altered immune regulation in the periphery and in the liver following
536 induction of SGVHD contributes to the development of the chronic inflammatory

responses described in the current manuscript. $CD4^+$ regulatory T cells have been shown to regulate the development of spontaneous and inducible murine colitis (3). Hess et al. have demonstrated that altered regulatory T cell activity contributed to the development of rat SGVHD with reduced numbers of regulatory lymphocytes being observed in diseased animals (24). Similarly, in a model of CsA-induced autoimmunity, it was shown that reconstitution of $CD4^+CD25^+$ regulatory T cells was delayed until after cessation of CsA treatment (62). With these findings in mind we have demonstrated that at the time of cessation of CsA therapy, significantly reduced numbers of $CD4^+CD25^+FoxP3^+$ T cells are present in the spleen and MLN of CsA-treated animals (J.S. Bryson, unpublished observations). Similar to the reduced expression of regulatory T cells in the SGVHD animal, results presented in the current manuscript demonstrated that another T cell population with regulatory potential, iNKT cells, was significantly reduced in the livers of SGVHD versus control BMT animals (Fig. 4E). Invariant NKT cells in the mouse express a single invariant Vα TCR chain (Vα14Jα18) (reviewed (31)), are positively selected to the nonclassical MHC molecule CD1d, have strong reactivity to the glycosphingolipid α-galactosylceramide (α-GalCer) and are present in high numbers in the liver. Liver iNKT cells have been shown to participate in the induction of oral tolerance (29, 57), tolerance to antigens in privileged sites (47) and inhibit the development of experimental colitis in mice (41, 46, 56). Significant reductions in $CD4^+$ Treg and iNKT are observed in the periphery and livers of SGVHD animals respectively. Thus, as a result of CsA therapy, reconstitution of these important regulatory immune populations is delayed and uncontrolled expansion of T effector cells occurs resulting in the development of chronic colon and ultimately, liver inflammation. In line with this hypothesis, we have demonstrated that recovery from SGVHD (approx.

30% of diseased animals) is associated with increases in regulatory T cells and iNKT cells and that $CD4^+CD25^+$ regulatory T cells from normal mice inhibited the adoptive transfer of SGVHD ((6) J. S. Bryson, unpublished observations) demonstrating the potential role of these cells in controlling chronic inflammation in this model system.

In other murine models of colitis the development of chronic liver inflammation was only observed in approximately 30% of mice (40). Significant and reproducible inflammatory liver lesions of bile ducts was observed in 100% of SGVHD mice in association with increased inflammatory mediators within the liver that are normally associated with colitis. Furthermore, significant changes in inflammatory markers associated with chronic liver inflammation were observed, suggesting a mechanistic relationship between the development of SGVHD- induced liver inflammation and that observed in the early stages of clinical disease. Similarities include the induction of inflammatory molecules that result in the influx of $CCR9^+$ $\beta7integrin^+$ $CD4^+$ T cells and inflammation of the intra and extrahepatic bile ducts. And while the model mimics many aspects of the disease process associated with clinical chronic liver inflammation, at the time points analyzed thus far, little to no sclerosis has been observed. Whether this is a limitation of the model or merely a timing issue in relation to disease induction remains to be elucidated. With the enterohepatic linkage and the previously published role of $CD4^+$ T cells in the SGVHD model (6, 10), the inflammatory response seen in these animals may provide an opportunity to study the pathobiology involved in both the initiation and progression of IBD-associated, chronic liver inflammation.

583 **GRANTS**

584

585 This work was supported by National Institutes of Health Grant PO1 CA092372 (J.S.B.).

586

587

FIGURE LEGENDS

Figure 1.

Histological examination of SGVHD livers showed development of chronic liver inflammation during murine SGVHD. To induce SGVHD C3H/HeN mice were lethally irradiated, reconstituted with syngeneic BM and treated daily for 21 days with CsA (15mg/kg/day) or the diluent olive oil. Tissues were taken when animals exhibited clinical symptoms (weight loss, diarrhea) of SGVHD-induced colitis (2-4 or 8 weeks post-CsA). (A) Control colon (H&E) demonstrating normal histology. (B) Colon from SGVHD animal (H&E) showing transmural inflammation with apoptotic cells, glandular invasion, crypt abscess formation and complete glandular destruction. Liver tissue from SGVHD animals (8 weeks post CsA) showing portal inflammation (D)(H&E) with focal extension beyond the limiting plate (E)(H&E),(F)(Trichrome) arrows. Transplant control liver (C)(H&E). Extra-hepatic bile ducts were isolated from control and SGVHD animals 3 weeks post CsA therapy. Control (G)(H&E) samples demonstrated mild surrounding inflammation of the common and branching bile duct. Samples of extra-hepatic bile ducts from SGVHD mice (H)(H&E) showed apoptotic changes in bile duct epithelium (small arrow) and invasion of bile duct epithelium by inflammatory cells in the common duct and branches. Inflammatory debris was present in the lumen and inflammatory cells in the surrounding adventitia. All tissues were photographed at 200X magnification.

Figure 2.

Increased colon and liver pathology associated with induction of SGVHD. Pathology grading of tissues was performed (9). Data represents mean grade ± SEM of samples from 2 experiments (n=9) and significance was determined using the unpaired Student's t test.

Figure 3.

Markers of chronic liver inflammation associated with SGVHD. Serum/plasma was isolated from BMT control or SGVHD mice 3-6 weeks after cessation of CsA therapy during active disease. Levels of ALT (A), anti-ssDNA (B) and p-ANCA (C) were determined as described in Methods. Left panels represent pooled data, mean ± SEM from 3 experiments collected at 2-6 weeks post CsA therapy. The data presented in right panels represents time course at time points after cessation of induction therapy (n=number of samples analyzed). Significance was determined using unpaired Student's t test, or Fisher's exact test, p-ANCA right panel.

Figure 4.

Increased $CD4^+$ T cell localization around the hepatic bile ducts in SGVHD livers. Liver associated mononuclear cells (LAM) were isolated from BMT control and SGVHD mice 2-4 weeks after cessation of CsA therapy. The percentage of $CD4^+$ and $CD8^+$ T cells (data from 5 pooled experiments) (A), percentage of CD4+ LAM that are β7 integrin+ or CCR9+ (B) (n=4 animals), iNKT (α-GalCer $CD1^+$ tetramer) (data from 3 pooled experiments normal n=2, control n= 3 and CsA n=6) (E) and $CD11b^+$ (F) (data from 4 pooled experiments) were determined by FACS analysis. Liver sections from transplant

control (C) and SGVHD mice (D) were examined by immunohistochemistry for presence of $CD4^+$ T cells. Significance was determined using unpaired Student's t test.

Figure 5

Increased levels of T_H1 and T_H17 immunity in the livers of SGVHD mice. At the time of active disease mice were euthanized, livers removed and pooled from 3-4 animals/experimental group. (A) LAM were isolated from the pooled liver preparations as described in the Methods Section, stimulated with anti-CD3 for 8 h with monensin being added during the last 4 h of culture. The cells were processed for intracellular cytokine staining of IL-17 and IFN-γ. Graphs represent mean ± SEM and is pooled data from 4 experiments. Significance determined using paired Student's t test. (B) Hepatic mRNA was extracted and cDNA prepared. Samples were analyzed for cytokine mRNA using real time RT-PCR for IL-23p19, IL-12p40 and TNF-α. Expression of these genes was normalized to GAPDH using the ΔΔCT method. Represents pooled data from 3 experiments, n=12 (IL-23p23, IL-12p40), n=8 (TNF-α) and significance was determined by unpaired Student's t test.

Figure 6.

Increased levels of liver inflammatory chemokines and adhesion molecules in SGVHD livers. Hepatic mRNA was extracted from SGVHD mice and cDNA prepared. Inflammatory chemokine and adhesion molecule mRNA was analyzed using real time RT-PCR for the primers CCL25, CCL28 CCR9 and MAdCAM-1. Expression of these genes was normalized to GAPDH using the ΔΔCT method. Represents pooled data

659 from 3 experiments, n=12 per group with significance determined using unpaired
660 Student's t test.
661
662 **Figure 7.**
663 *CD4$^+$ T cells migrate to the liver after cessation of CsA therapy*. Livers were isolated at
664 14, 21 and 37 days from SGVHD and control animals and analyzed (A) by
665 immunohistochemistry for the presence of CD4$^+$ T cells or (B) for MAdCAM mRNA 21
666 days after BMT by real time RT-PCR. Data presented representative of (A) 4 tissues
667 from two experiments, (B) or pooled samples (mean ± SEM) from two experiments, n=8
668 and were analyzed using unpaired Student's t test.
669
670 **Figure 8.**
671 *LAM from SGVHD livers showed an increase proliferative response to CeAg-pulsed DC.*
672 Liver associated mononuclear cells (LAM) were isolated from BMT control and SGVHD
673 mice four weeks after cessation of CsA therapy. Proliferation against CeAg-pulsed DC
674 in the presence or absence of anti-CD4 mAb was measured by thymidine incorporation
675 during the last 18 to 96 h assay. Data comparing CeAg-induced proliferation
676 representative of 3 experiments and represents mean ± SEM of triplicate samples and
677 significance was determined using unpaired Student's t test. CD4 blocking represents
678 results from a single experiment. *Different from control LAM stimulated with DC-CeAg
679 p=0.0209. **Different from SGVHD DC-Ag p=0.0231
680
681

SUPPLEMENTAL FIGURE LEGENDS

Supplemental Figure 1.

SGVHD mice showed increased liver TLR mRNA. SGVHD was induced as described. At 2-4 weeks post-CsA mice were euthanized and their livers removed. Hepatic mRNA was extracted and cDNA prepared. Samples were analyzed using real time RT-PCR for the primers TLR 2,4,5 & 9 (A-D respectively) and the expression of these genes was normalized to GAPDH using the ΔΔCT method. Represents pooled data from 3 experiments, n=12 per group and significance was determined using unpaired Student's t test.

Supplemental Figure 2.

Increased TLR expression in LAM isolated from SGVHD. LAM were isolated from 2-4 weeks post-CsA therapy from 2-4 control and SGVHD animals and pooled within each treatment group. The cells were stained for the surface and intracellular expression of CD11b and TLR2 and TLR5. RAW264.7 cells were utilized as positive control for TLR staining and were positive for TLR2. A. Representative flow diagrams for staining of TLR2 and TLR5. B. Pooled results from three experiments analyzing expression of TLR2 and TLR5 in LAM from control and SGVHD mice. Significance determined using unpaired Student's t test.

REFERENCES.

1. Adams DH, and Eksteen B. Aberrant homing of mucosal T cells and extra-intestinal manifestations of inflammatory bowel disease. *Nat Rev Immunol* 6: 244-251, 2006.

2. Agace WW. Tissue-tropic effector T cells: generation and targeting opportunities. *Nat Rev Immunol* 6: 682-692, 2006.

3. Asseman C, Fowler S, and Powrie F. Control of experimental inflammatory bowel disease by regulatory T cells. *Am J Respir Crit Care Med* 162: S185-189., 2000.

4. Bondada S, Bikah G, Robertson DA, and Sen G. Role of CD5 in growth regulation of B-1 cells. *Curr Top Microbiol Immunol* 252: 141-149, 2000.

5. Broome U, Olsson R, Loof L, Bodemar G, Hultcrantz R, Danielsson A, Prytz H, Sandberg-Gertzen H, Wallerstedt S, and Lindberg G. Natural history and prognostic factors in 305 Swedish patients with primary sclerosing cholangitis. *Gut* 38: 610-615, 1996.

6. Bryson JS, Jennings CD, Brandon JA, Perez J, Caywood BE, and Kaplan AM. Adoptive transfer of murine syngeneic graft-vs.-host disease by CD4+ T cells. *J Leukoc Biol* 82: 1393-1400, 2007.

7. Bryson JS, Jennings CD, Caywood BE, and Kaplan AM. Induction of a syngeneic graft-versus-host disease-like syndrome in DBA/2 mice. *Transplantation* 48: 1042-1047., 1989.

8. Bryson JS, Jennings CD, Caywood BE, and Kaplan AM. Thy1+ bone marrow cells regulate the induction of murine syngeneic graft-versus-host disease. *Transplantation* 56: 941-945, 1993.

9. Bryson JS, Jennings CD, Lowery DM, Carlson SL, Pflugh DL, Caywood BE, and Kaplan AM. Rejection of an MHC class II negative tumor following induction of murine syngeneic graft-versus-host disease. *Bone Marrow Transplant* 23: 363-372, 1999.

10. Bryson JS, Zhang L, Goes SW, Jennings CD, Caywood BE, Carlson SL, and Kaplan AM. CD4+ T cells mediate murine syngeneic graft-versus-host disease-associated colitis. *J Immunol* 172: 679-687, 2004.

11. Buxbaum J, Qian P, Allen PM, and Peters MG. Hepatitis resulting from liver-specific expression and recognition of self-antigen. *J Autoimmun* 31: 208-215, 2008.

12. Chung BH, Li C, Sun BK, Lim SW, Ahn KO, Yang JH, Choi YH, Yoon KH, Sugawara A, Ito S, Kim J, and Yang CW. Rosiglitazone protects against cyclosporine-induced pancreatic and renal injury in rats. *Am J Transplant* 5: 1856-1867, 2005.

13. Cong Y, Brandwein SL, McCabe RP, Lazenby A, Birkenmeier EH, Sundberg JP, and Elson CO. CD4+ T cells reactive to enteric bacterial antigens in spontaneously colitic C3H/HeJBir mice: increased T helper cell type 1 response and ability to transfer disease. *J Exp Med* 187: 855-864, 1998.

14. Corsini E, Viviani B, Marinovich M, and Galli CL. Cyclosporin A exacerbates skin irritation induced by tributyltin by increasing nuclear factor kappa B activation. *J Invest Dermatol* 117: 1627-1634, 2001.

15. Diehl AM, Li ZP, Lin HZ, and Yang SQ. Cytokines and the pathogenesis of non-alcoholic steatohepatitis. *Gut* 54: 303-306, 2005.

16. Eksteen B, Miles AE, Grant AJ, and Adams DH. Lymphocyte homing in the pathogenesis of extra-intestinal manifestations of inflammatory bowel disease. *Clin Med* 4: 173-180, 2004.

17. Farrant JM, Hayllar KM, Wilkinson ML, Karani J, Portmann BC, Westaby D, and Williams R. Natural history and prognostic variables in primary sclerosing cholangitis. *Gastroenterology* 100: 1710-1717, 1991.

18. Flanagan DL, Gross R, Jennings CD, Caywood BE, Goes S, Kaplan AM, and Bryson JS. Induction of syngeneic graft-versus-host disease in LPS hyporesponsive C3H/HeJ mice. *J Leukoc Biol* 70: 873-880, 2001.

19. Flanagan DL, Jennings CD, and Bryson JS. Th1 cytokines and NK cells participate in the development of murine syngeneic graft-versus-host disease. *J Immunol* 163: 1170-1177, 1999.

20. Fujino S, Andoh A, Bamba S, Ogawa A, Hata K, Araki Y, Bamba T, and Fujiyama Y. Increased expression of interleukin 17 in inflammatory bowel disease. *Gut* 52: 65-70, 2003.

21. Giulietti A, Overbergh L, Valckx D, Decallonne B, Bouillon R, and Mathieu C. An overview of real-time quantitative PCR: applications to quantify cytokine gene expression. *Methods* 25: 386-401, 2001.

22. Harada K, Shimoda S, Sato Y, Isse K, Ikeda H, and Nakanuma Y. Periductal interleukin-17 production in association with biliary innate immunity contributes to the pathogenesis of cholangiopathy in primary biliary cirrhosis. *Clin Exp Immunol* 157: 261-270, 2009.

775 **23. Harrington LE, Mangan PR, and Weaver CT. Expanding the effector CD4 T-**
776 **cell repertoire: the Th17 lineage. *Curr Opin Immunol* 18: 349-356, 2006.**
777 **24. Hess AD, and Thoburn CJ. Immune tolerance to self-major**
778 **histocompatibility complex class II antigens after bone marrow transplantation:**
779 **role of regulatory T cells. *Biol Blood Marrow Transplant* 12: 518-529, 2006.**
780 **25. Hill GR, Crawford JM, Cooke KR, Brinson YS, Pan L, and Ferrara JL. Total**
781 **body irradiation and acute graft-versus-host disease: the role of gastrointestinal**
782 **damage and inflammatory cytokines. *Blood* 90: 3204-3213, 1997.**
783 **26. Hillan KJ, Hagler KE, MacSween RN, Ryan AM, Renz ME, Chiu HH, Ferrier**
784 **RK, Bird GL, Dhillon AP, Ferrell LD, and Fong S. Expression of the mucosal**
785 **vascular addressin, MAdCAM-1, in inflammatory liver disease. *Liver* 19: 509-518,**
786 **1999.**
787 **27. Holtta V, Klemetti P, Sipponen T, Westerholm-Ormio M, Kociubinski G, Salo**
788 **H, Rasanen L, Kolho KL, Farkkila M, Savilahti E, and Vaarala O. IL-23/IL-17**
789 **immunity as a hallmark of Crohn's disease. *Inflamm Bowel Dis* 14: 1175-1184,**
790 **2008.**
791 **28. Iwasaki A, and Medzhitov R. Toll-like receptor control of the adaptive**
792 **immune responses. *Nat Immunol* 5: 987-995, 2004.**
793 **29. Kim HJ, Hwang SJ, Kim BK, Jung KC, and Chung DH. NKT cells play**
794 **critical roles in the induction of oral tolerance by inducing regulatory T cells**
795 **producing IL-10 and transforming growth factor beta, and by clonally deleting**
796 **antigen-specific T cells. *Immunology* 118: 101-111, 2006.**
797 **30. Knight C, and Murray KF. Hepatobiliary associations with inflammatory**
798 **bowel disease. *Expert Rev Gastroenterol Hepatol* 3: 681-691, 2009.**

31. Kronenberg M, and Gapin L. The unconventional lifestyle of NKT cells. *Nat Rev Immunol* 2: 557-568, 2002.

32. Lafdil F, Wang H, Park O, Zhang W, Moritoki Y, Yin S, Fu XY, Gershwin ME, Lian ZX, and Gao B. Myeloid STAT3 inhibits T cell-mediated hepatitis by regulating T helper 1 cytokine and interleukin-17 production. *Gastroenterology* 137: 2125-2135 e2121-2122, 2009.

33. Lan RY, Salunga TL, Tsuneyama K, Lian ZX, Yang GX, Hsu W, Moritoki Y, Ansari AA, Kemper C, Price J, Atkinson JP, Coppel RL, and Gershwin ME. Hepatic IL-17 responses in human and murine primary biliary cirrhosis. *J Autoimmun* 32: 43-51, 2009.

34. LaSpina M, Tripathi S, Gatto LA, Bruch D, Maier KG, and Kittur DS. An interleukin-6-neutralizing antibody prevents cyclosporine-induced nephrotoxicity in mice. *J Surg Res* 148: 121-125, 2008.

35. Lichtman SN, Keku J, Clark RL, Schwab JH, and Sartor RB. Biliary tract disease in rats with experimental small bowel bacterial overgrowth. *Hepatology* 13: 766-772, 1991.

36. Lichtman SN, Wang J, and Clark RL. A microcholangiographic study of liver disease models in rats. *Acad Radiol* 2: 515-521, 1995.

37. Lohr J, Knoechel B, Wang JJ, Villarino AV, and Abbas AK. Role of IL-17 and regulatory T lymphocytes in a systemic autoimmune disease. *J Exp Med* 203: 2785-2791, 2006.

38. Matsuda JL, Naidenko OV, Gapin L, Nakayama T, Taniguchi M, Wang CR, Koezuka Y, and Kronenberg M. Tracking the response of natural killer T cells to a glycolipid antigen using CD1d tetramers. *J Exp Med* 192: 741-754, 2000.

39. Mendes FD, Levy C, Enders FB, Loftus EV, Jr., Angulo P, and Lindor KD. Abnormal hepatic biochemistries in patients with inflammatory bowel disease. *The American journal of gastroenterology* 102: 344-350, 2007.

40. Numata Y, Tazuma S, Nishioka T, Ueno Y, and Chayama K. Immune response in mouse experimental cholangitis associated with colitis induced by dextran sulfate sodium. *J Gastroenterol Hepatol* 19: 910-915, 2004.

41. Numata Y, Tazuma S, Ueno Y, Nishioka T, Hyogo H, and Chayama K. Therapeutic effect of repeated natural killer T cell stimulation in mouse cholangitis complicated by colitis. *Dig Dis Sci* 50: 1844-1851, 2005.

42. O'Mahony CA, and Vierling JM. Etiopathogenesis of primary sclerosing cholangitis. *Semin Liver Dis* 26: 3-21, 2006.

43. Orth T, Peters M, Schlaak JF, Krummenauer F, Wanitschke R, Mayet WJ, Galle PR, and Neurath MF. Mycophenolate mofetil versus azathioprine in patients with chronic active ulcerative colitis: a 12-month pilot study. *The American journal of gastroenterology* 95: 1201-1207., 2000.

44. Overbergh L, Valckx D, Waer M, and Mathieu C. Quantification of murine cytokine mRNAs using real time quantitative reverse transcriptase PCR. *Cytokine* 11: 305-312, 1999.

45. Rong G, Zhou Y, Xiong Y, Zhou L, Geng H, Jiang T, Zhu Y, Lu H, Zhang S, Wang P, Zhang B, and Zhong R. Imbalance between T helper type 17 and T regulatory cells in patients with primary biliary cirrhosis: the serum cytokine profile and peripheral cell population. *Clin Exp Immunol* 156: 217-225, 2009.

46. Shlomai A, Trop S, Gotsman I, Jurim O, Diment J, Alper R, Rabbani E, Engelhardt D, and Ilan Y. Immunomodulation of experimental colitis: the role of NK1.1 liver lymphocytes and surrogate antigens--bystander effect. *J Pathol* 195: 498-507, 2001.

47. Sonoda KH, Exley M, Snapper S, Balk SP, and Stein-Streilein J. CD1-reactive natural killer T cells are required for development of systemic tolerance through an immune-privileged site. *J Exp Med* 190: 1215-1226, 1999.

48. Strober W, Fuss I, and Mannon P. The fundamental basis of inflammatory bowel disease. *J Clin Invest* 117: 514-521, 2007.

49. Strober W, Fuss IJ, and Blumberg RS. The immunology of mucosal models of inflammation. *Annu Rev Immunol* 20: 495-549, 2002.

50. Talwalkar JA, and Lindor KD. Primary sclerosing cholangitis. *Inflamm Bowel Dis* 11: 62-72, 2005.

51. Tariq M, Morais C, Sobki S, Al Sulaiman M, and Al Khader A. N-acetylcysteine attenuates cyclosporin-induced nephrotoxicity in rats. *Nephrol Dial Transplant* 14: 923-929, 1999.

52. Terjung B, Soehne J, Lechtenberg B, Gottwein J, Muennich M, Herzog V, Maehler M, Sauerbruch T, and Spengler U. p-ANCA in Autoimmune Liver Disorders Recognize Human Beta-Tubulin Isotype 5 and Cross-react with Microbial Protein FtsZ. *Gut* 2009.

53. Terjung B, and Spengler U. Atypical p-ANCA in PSC and AIH: a hint toward a "leaky gut"? *Clin Rev Allergy Immunol* 36: 40-51, 2009.

54. Terjung B, and Spengler U. Role of auto-antibodies for the diagnosis of chronic cholestatic liver diseases. *Clin Rev Allergy Immunol* 28: 115-133, 2005.

55. Toyonaga T, Hino O, Sugai S, Wakasugi S, Abe K, Shichiri M, and Yamamura K. Chronic active hepatitis in transgenic mice expressing interferon-gamma in the liver. *Proc Natl Acad Sci U S A* 91: 614-618, 1994.

56. Trop S, and Ilan Y. NK 1.1+ T cell: a two-faced lymphocyte in immune modulation of the IL-4/IFN-gamma paradigm. *J Clin Immunol* 22: 270-280, 2002.

57. Trop S, Samsonov D, Gotsman I, Alper R, Diment J, and Ilan Y. Liver-associated lymphocytes expressing NK1.1 are essential for oral immune tolerance induction in a murine model. *Hepatology* 29: 746-755, 1999.

58. Vierling JM, Ruderman WB, Jaffee BD, Fennell RH, Jr., and Claman HN. Hepatic lesions in murine chronic graft-versus-host disease to minor histocompatibility antigens. A reproducible model of nonsuppurative destructive cholangitis. *Transplantation* 48: 717-718, 1989.

59. Wakabayashi K, Lian ZX, Moritoki Y, Lan RY, Tsuneyama K, Chuang YH, Yang GX, Ridgway W, Ueno Y, Ansari AA, Coppel RL, Mackay IR, and Gershwin ME. IL-2 receptor alpha(-/-) mice and the development of primary biliary cirrhosis. *Hepatology* 44: 1240-1249, 2006.

60. Wolf A, Trendelenburg CF, Diez-Fernandez C, Prieto P, Houy S, Trommer WE, and Cordier A. Cyclosporine A-induced oxidative stress in rat hepatocytes. *J Pharmacol Exp Ther* 280: 1328-1334, 1997.

61. Worthington J, Cullen S, and Chapman R. Immunopathogenesis of primary sclerosing cholangitis. *Clin Rev Allergy Immunol* 28: 93-103, 2005.

62. Wu DY, and Goldschneider I. Cyclosporin A-induced autologous graft-versus-host disease: a prototypical model of autoimmunity and active (dominant) tolerance coordinately induced by recent thymic emigrants. *J Immunol* 162: 6926-6933., 1999.

63. Xun CQ, Thompson JS, Jennings CD, Brown SA, and Widmer MB. Effect of total body irradiation, busulfan-cyclophosphamide, or cyclophosphamide conditioning on inflammatory cytokine release and development of acute and chronic graft-versus-host disease in H-2-incompatible transplanted SCID mice. *Blood* 83: 2360-2367, 1994.

64. Zhou D, Brown SA, Yu T, Chen G, Barve S, Kang BC, and Thompson JS. A high dose of ionizing radiation induces tissue-specific activation of nuclear factor-kappaB in vivo. *Radiat Res* 151: 703-709, 1999.

FIGURES

Figure 1.

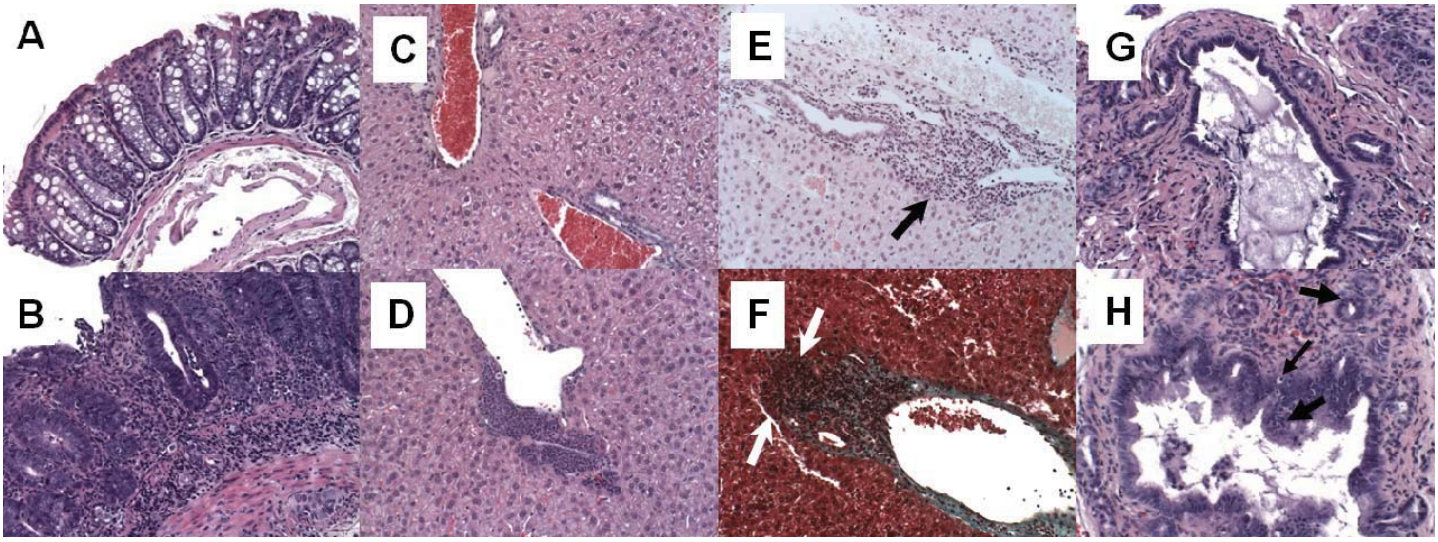

Figure 2

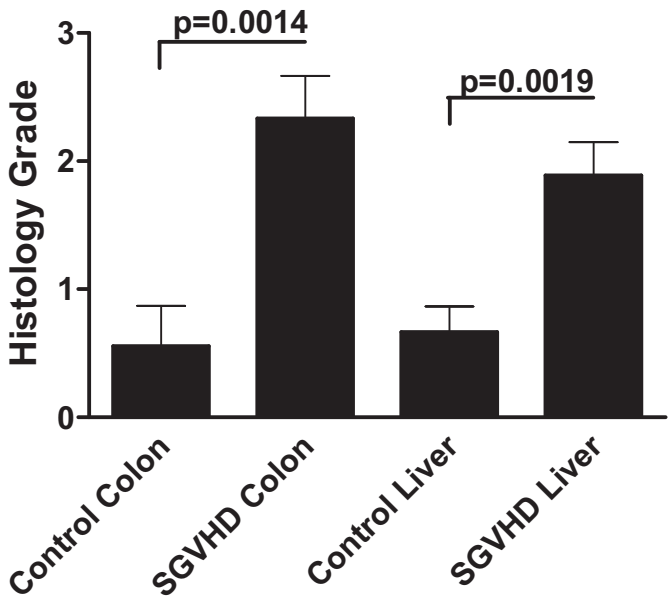
p=0.0014
p=0.0019
Histology Grade
3
2
1
0
Control Colon
SGVHD Colon
Control Liver
SGVHD Liver

Figure 3.

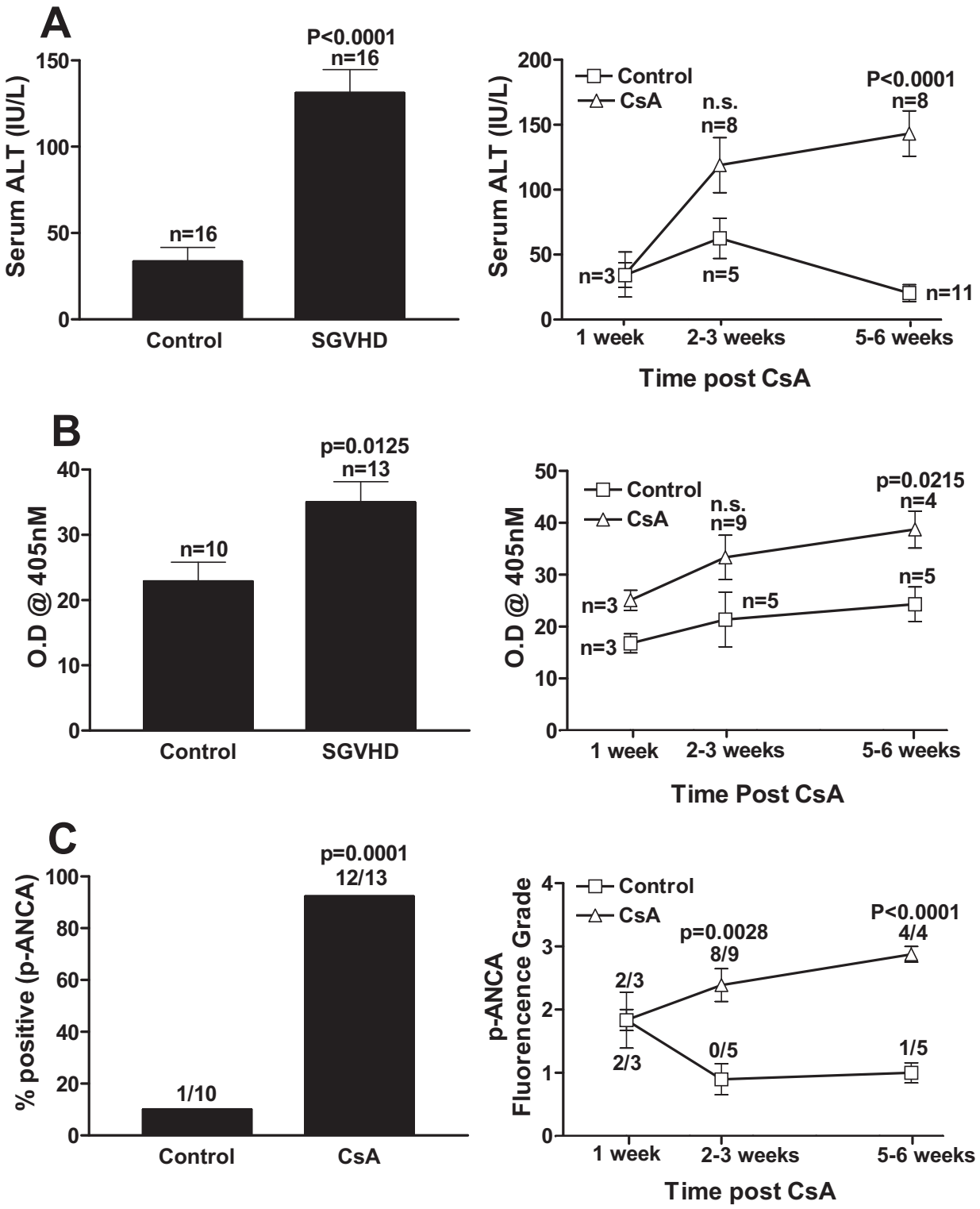
A
Serum ALT (IU/L)
150
100
50
0
n=16
P<0.0001
n=16
Control
SGVHD
Serum ALT (IU/L)
200
150
100
50
0
Control
CsA
n.s.
n=8
P<0.0001
n=8
n=3
n=5
n=11
1 week
2-3 weeks
5-6 weeks
Time post CsA
B
O.D @ 405nM
40
30
20
10
0
n=10
p=0.0125
n=13
Control
SGVHD
O.D @ 405nM
50
40
30
20
10
0
Control
CsA
n.s.
n=9
p=0.0215
n=4
n=3
n=5
n=3
n=5
1 week
2-3 weeks
5-6 weeks
Time Post CsA
C
% positive (p-ANCA)
100
80
60
40
20
0
1/10
p=0.0001
12/13
Control
CsA
p-ANCA
Fluorencence Grade
4
3
2
1
0
Control
CsA
p=0.0028
8/9
P<0.0001
4/4
2/3
2/3
0/5
1/5
1 week
2-3 weeks
5-6 weeks
Time post CsA

Figure 4

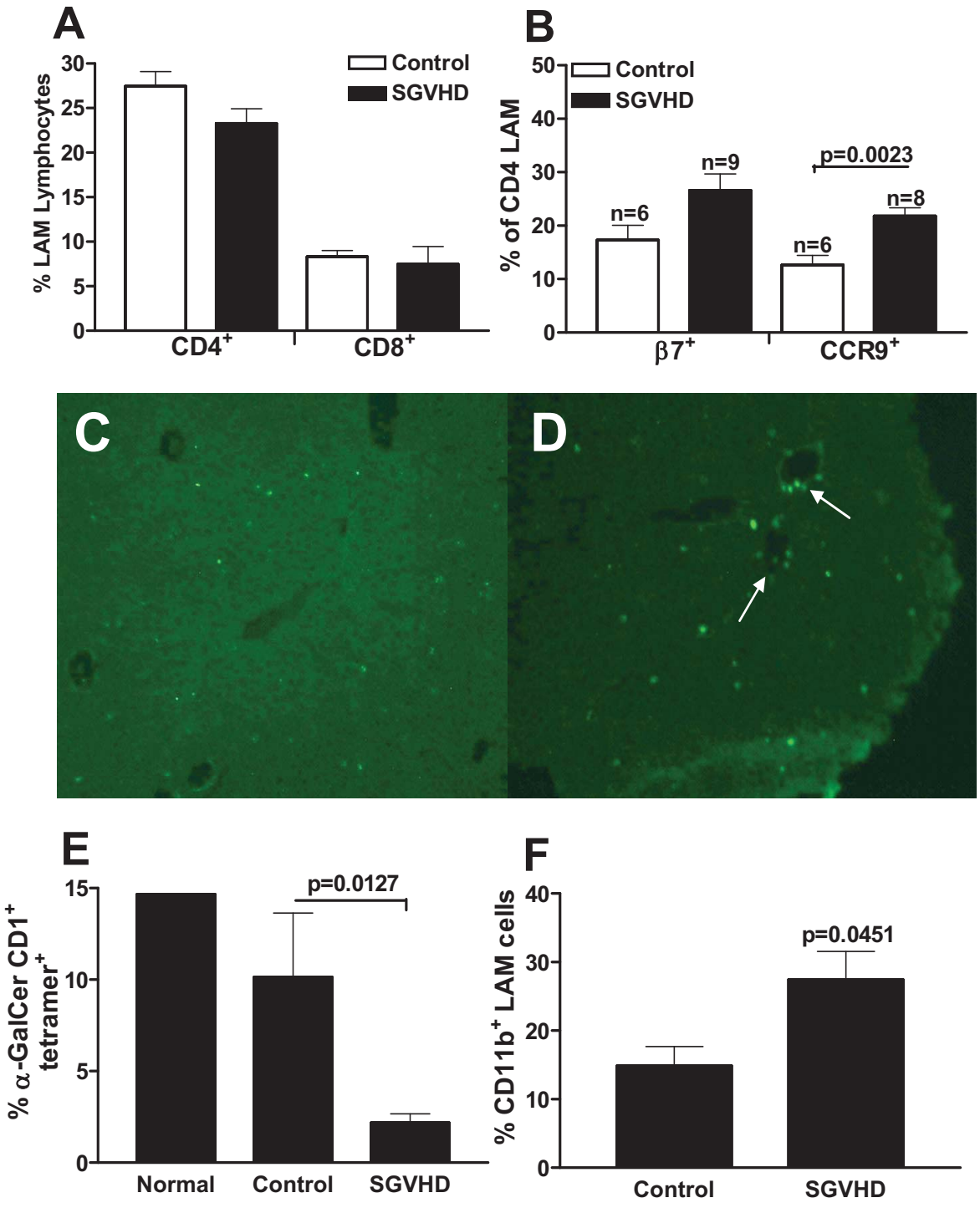
A
% LAM Lymphocytes
30
25
20
15
10
5
0
Control
SGVHD
CD4+
CD8+
B
% of CD4 LAM
50
40
30
20
10
0
Control
SGVHD
n=6
n=9
p=0.0023
n=6
n=8
β7+
CCR9+
C
D
E
% α-GalCer CD1+ tetramer+
15
10
5
0
p=0.0127
Normal
Control
SGVHD
F
% CD11b+ LAM cells
40
30
20
10
0
p=0.0451
Control
SGVHD

Figure 5

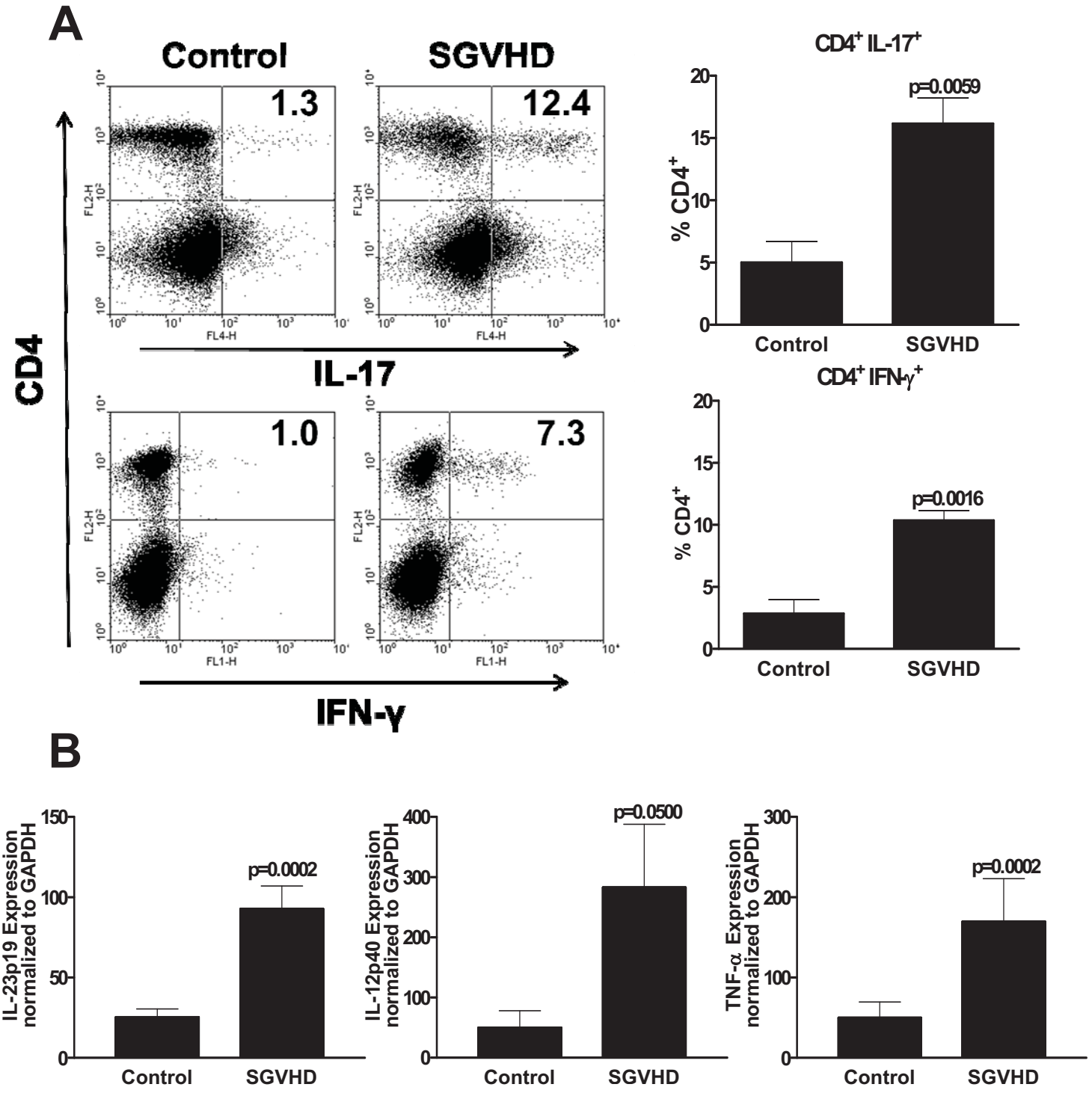
A
Control
SGVHD
1.3
12.4
1.0
7.3
CD4
IL-17
IFN-γ
FL2-H
FL4-H
FL1-H
CD4+ IL-17+
% CD4+
p=0.0059
Control
SGVHD
CD4+ IFN-γ+
p=0.0016
B
IL-23p19 Expression normalized to GAPDH
p=0.0002
IL-12p40 Expression normalized to GAPDH
p=0.0500
TNF-α Expression normalized to GAPDH
p=0.0002

Figure 6

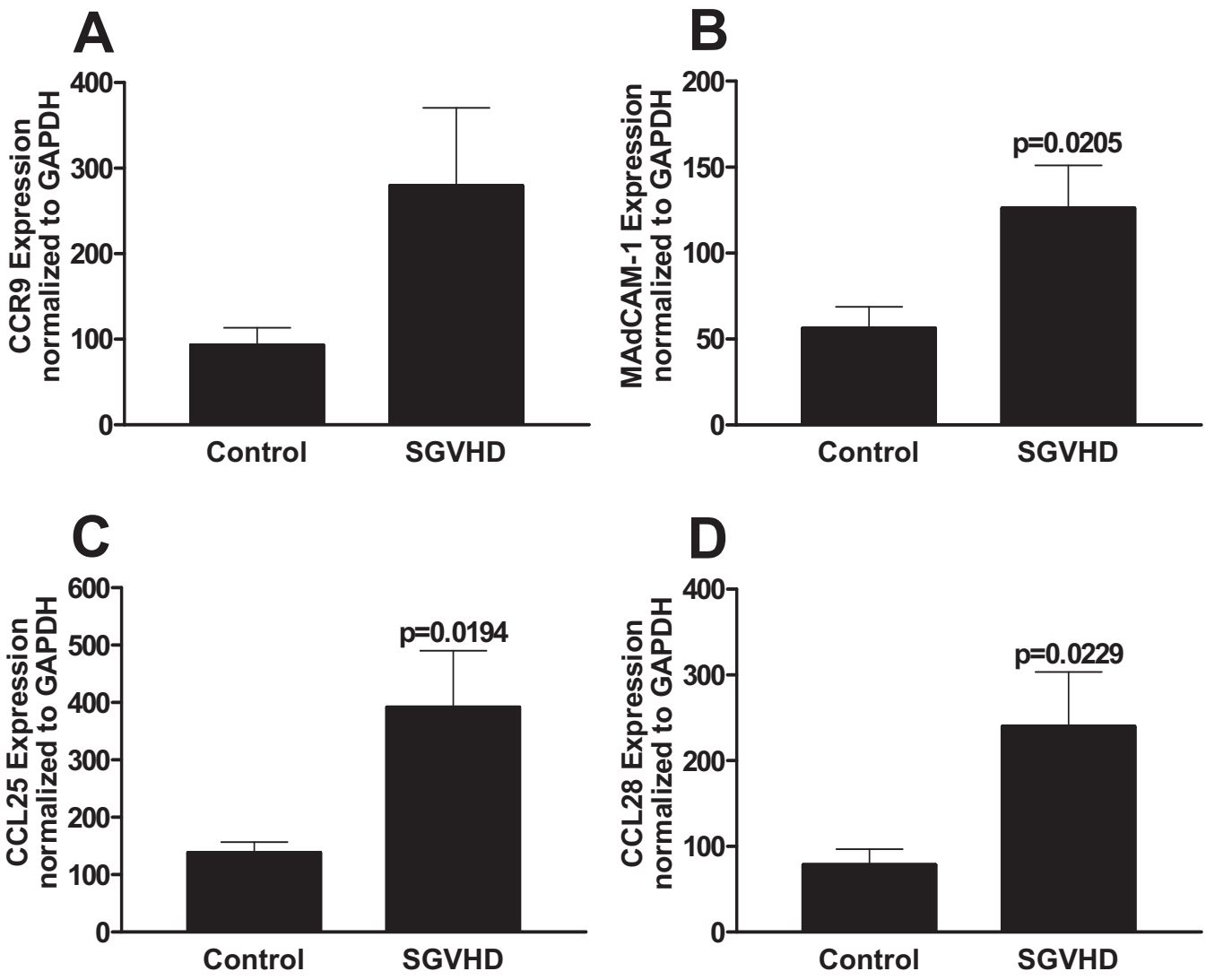
A
CCR9 Expression normalized to GAPDH
400
300
200
100
0
Control
SGVHD
B
MAdCAM-1 Expression normalized to GAPDH
200
150
100
50
0
p=0.0205
Control
SGVHD
C
CCL25 Expression normalized to GAPDH
600
500
400
300
200
100
0
p=0.0194
Control
SGVHD
D
CCL28 Expression normalized to GAPDH
400
300
200
100
0
p=0.0229
Control
SGVHD

Figure 7

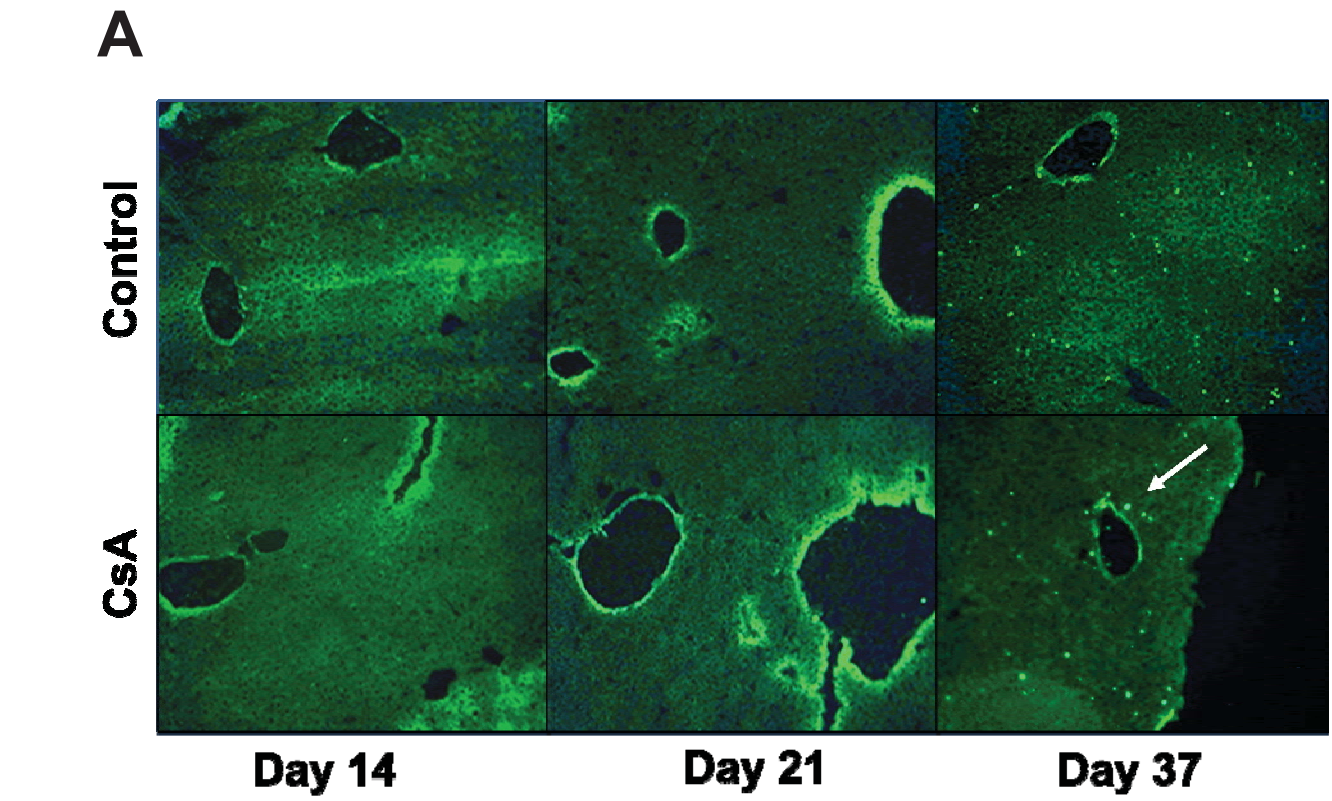
A
Control
CsA
Day 14
Day 21
Day 37

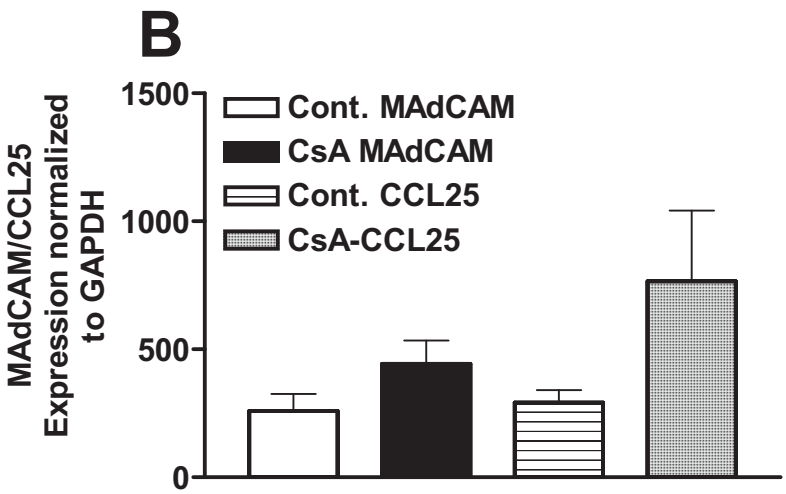
B
MAdCAM/CCL25
Expression normalized
to GAPDH
1500
1000
500
0
Cont. MAdCAM
CsA MAdCAM
Cont. CCL25
CsA-CCL25

Figure 8.

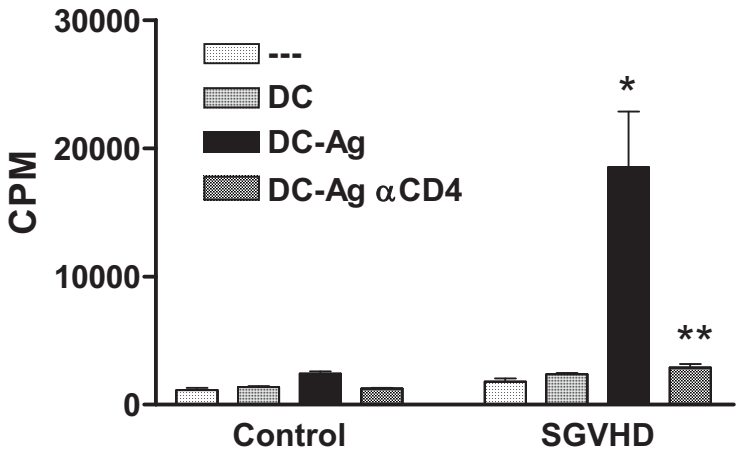

Supplemental Figure 1

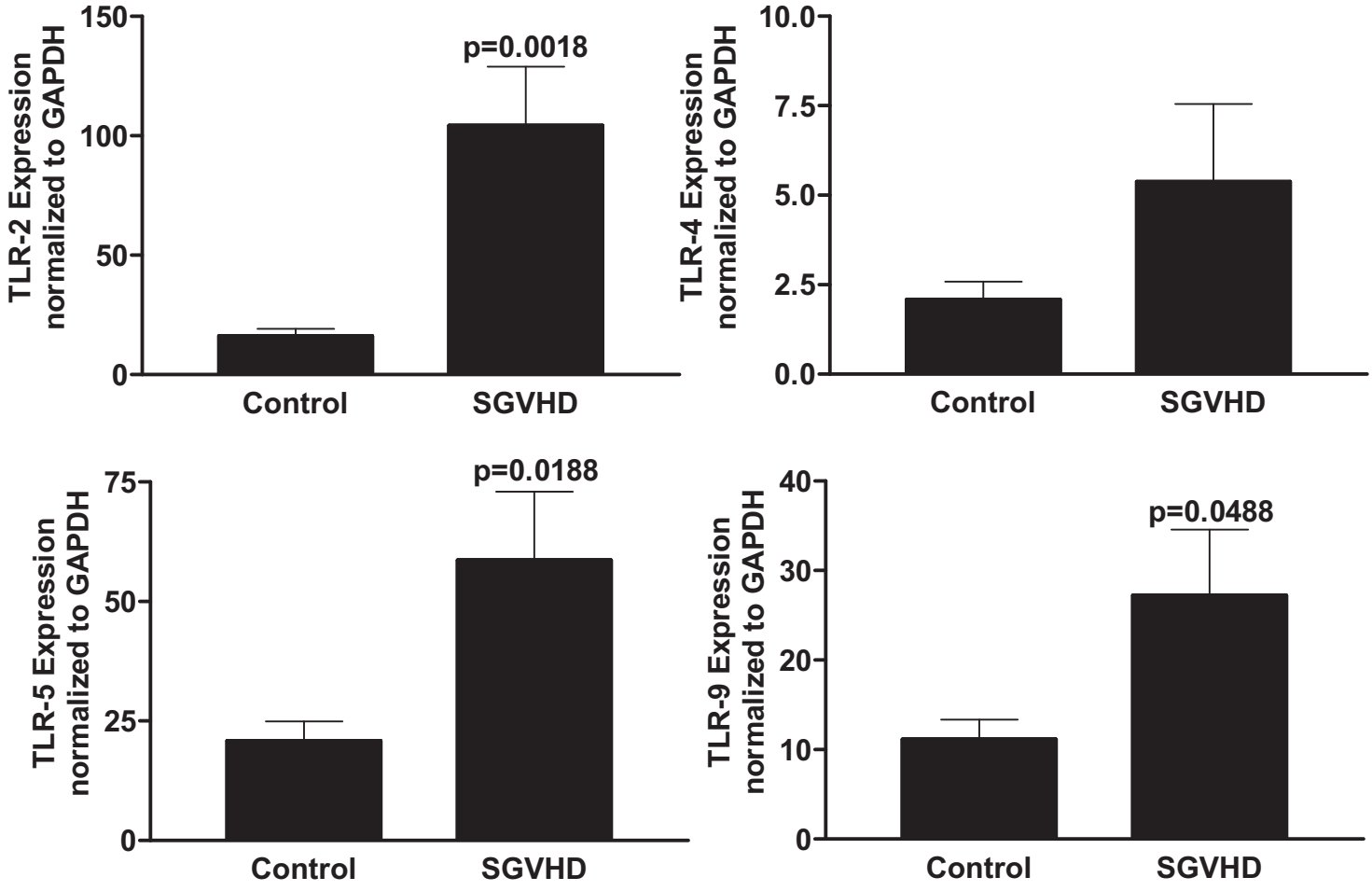

Supplemental Figure 2.